Adversarial Examples Can Be Effective Data Augmentation for Unsupervised Machine Learning

Chia-Yi Hsu[1], Pin-Yu Chen[2], Songtao Lu[2], Sijia Liu[3], Chia-Mu Yu[1]
[1]National Yang Ming Chiao Tung University
[2] IBM Research
[3] Michigan State University
{chiayihsu8315, chiamuyu}@gmail.com, {pin-yu.chen, songtao}@ibm.com, liusiji5@msu.edu

Abstract

Adversarial examples causing evasive predictions are widely used to evaluate and improve the robustness of machine learning models. However, current studies focus on supervised learning tasks, relying on the ground-truth data label, a targeted objective, or supervision from a trained classifier. In this paper, we propose a framework of generating adversarial examples for **unsupervised** models and demonstrate novel applications to data augmentation. Our framework exploits a mutual information neural estimator as an information-theoretic similarity measure to generate adversarial examples without supervision. We propose a new MinMax algorithm with provable convergence guarantees for efficient generation of unsupervised adversarial examples. Our framework can also be extended to supervised adversarial examples. When using unsupervised adversarial examples as a simple plug-in data augmentation tool for model retraining, significant improvements are consistently observed across different unsupervised tasks and datasets, including data reconstruction, representation learning, and contrastive learning. Our results show novel methods and considerable advantages in studying and improving unsupervised machine learning via adversarial examples.

1 Introduction

Adversarial examples are known as prediction-evasive attacks on state-of-the-art machine learning models (e.g., deep neural networks), which are often generated by manipulating native data samples while maintaining high similarity measured by task-specific metrics such as L_p-norm bounded perturbations (Goodfellow, Shlens, and Szegedy 2015; Biggio and Roli 2018). Due to the implications and consequences on mission-critical and security-centric machine learning tasks, adversarial examples are widely used for robustness evaluation of a trained model and for robustness enhancement during training (i.e., adversarial training).

Despite of a plethora of adversarial attacking algorithms, the design principle of existing methods is primarily for *supervised* learning models — requiring either the true label or a targeted objective (e.g., a specific class label or a reference sample). Some recent works have extended to the *semi-supervised* setting, by leveraging supervision from a classifier (trained on labeled data) and using the predicted labels on unlabeled data for generating (semi-supervised) adversarial examples (Miyato et al. 2018; Zhang et al. 2019; Stanforth et al. 2019; Carmon et al. 2019). On the other hand, recent advances in unsupervised and few-shot machine learning techniques show that task-invariant representations can be learned and contribute to downstream tasks with limited or even without supervision (Ranzato et al. 2007; Zhu and Goldberg 2009; Zhai et al. 2019), which motivates this study regarding their robustness. Our goal is to provide efficient robustness evaluation and data augmentation techniques for unsupervised (and self-supervised) machine learning models through *unsupervised* adversarial examples (UAEs). Table 1 summarizes the fundamental difference between conventional supervised adversarial examples and our UAEs. Notably, our UAE generation is supervision-free because it solely uses an information-theoretic similarity measure and the associated unsupervised learning objective function. It does not use any supervision such as label information or prediction from other supervised models.

(I) *Mathematical notation*	
$M^{\text{sup}}/M^{\text{unsup}}$: trained supervised/unsupervised machine learning models x/x_{adv}: original/adversarial data sample $\ell_x^{\text{sup}}/\ell_x^{\text{unsup}}$: supervised/unsupervised loss function in reference to x	
(II) *Supervised tasks* (e.g. classification)	(III) ***Unsupervised tasks*** (our proposal) (e.g. data reconstruction, contrastive learning)
x_{adv} is **similar** to x but $M^{\text{sup}}(x_{\text{adv}}) \neq M^{\text{sup}}(x)$	x_{adv} is **dissimilar** to x but $\ell_x^{\text{unsup}}(x_{\text{adv}}\|M^{\text{unsup}}) \leq \ell_x^{\text{unsup}}(x\|M^{\text{unsup}})$

Table 1: Illustration of adversarial examples for supervised/unsupervised machine learning tasks. Both settings use a native data sample x as reference. For supervised setting, adversarial examples refer to *similar* samples of x causing inconsistent predictions. For unsupervised setting, adversarial examples refer to *dissimilar* samples yielding smaller loss than x, relating to generalization errors on low-loss samples.

Copyright © 2022, Association for the Advancement of Artificial Intelligence (www.aaai.org). All rights reserved.

In this paper, we aim to formalize the notion of UAE, establish an efficient framework for UAE generation, and demonstrate the advantage of UAEs for improving a variety of unsupervised machine learning tasks. We summarize our main contributions as follows.

• We propose a new per-sample based mutual information neural estimator (MINE) between a pair of original and modified data samples as an information-theoretic similarity measure and a supervision-free approach for generating UAE. For instance, see UAEs for data reconstruction in Figure **??** of supplementary material. While our primary interest is generating adversarial examples for unsupervised learning models, we also demonstrate that our per-sample MINE can be used to generate adversarial examples for supervised learning models with improved visual quality.

• We formulate the generation of adversarial examples with MINE as a constrained optimization problem, which applies to both supervised and unsupervised machine learning tasks. We then develop an efficient MinMax optimization algorithm (Algorithm 1) and prove its convergence. We also demonstrate the advantage of our MinMax algorithm over the conventional penalty-based method.

• We show a novel application of UAEs as a simple plug-in data augmentation tool for several unsupervised machine learning tasks, including data reconstruction, representation learning, and contrastive learning on image and tabular datasets. Our extensive experimental results show outstanding performance gains (up to 73.5% performance improvement) by retraining the model with UAEs.

2 Related Work and Background

2.1 Adversarial Attack and Defense

For supervised adversarial examples, the attack success criterion can be either *untargeted* (i.e. model prediction differs from the true label of the corresponding native data sample) or *targeted* (i.e. model prediction targeting a particular label or a reference sample). In addition, a similarity metric such as L_p-norm bounded perturbation is often used when generating adversarial examples. The projected gradient descent (PGD) attack (Madry et al. 2018) is a widely used approach to find L_p-norm bounded supervised adversarial examples. Depending on the attack threat model, the attacks can be divided into white-box (Szegedy et al. 2013; Carlini and Wagner 2017b), black-box (Chen et al. 2017; Brendel, Rauber, and Bethge 2018; Liu et al. 2020), and transfer-based (Nitin Bhagoji et al. 2018; Papernot et al. 2017) approaches.

Although a plethora of defenses were proposed, many of them failed to withstand advanced attacks (Carlini and Wagner 2017a; Athalye, Carlini, and Wagner 2018). Adversarial training (Madry et al. 2018) and its variants aiming to generate worst-case adversarial examples during training are so far the most effective defenses. However, adversarial training on supervised adversarial examples can suffer from undesirable tradeoff between robustness and accuracy (Su et al. 2018; Tsipras et al. 2019). Following the formulation of untargeted supervised attacks, recent studies such as (Cemgil et al. 2020) generate adversarial examples for unsupervised tasks by finding an adversarial example within an L_p-norm perturbation constraint that maximizes the training loss. In contrast, our approach aims to find adversarial examples that have low training loss but are dissimilar to the native data (see Table 1), which plays a similar role to the category of "on-manifold" adversarial examples governing generalization errors (Stutz, Hein, and Schiele 2019). In supervised setting, (Stutz, Hein, and Schiele 2019) showed that adversarial training with L_p-norm constrained perturbations may find off-manifold adversarial examples and hurt generalization.

2.2 Mutual Information Neural Estimator

Mutual information (MI) measures the mutual dependence between two random variables X and Z, defined as $I(X,Z) = H(X) - H(X|Z)$, where $H(X)$ denotes the (Shannon) entropy of X and $H(X|Z)$ denotes the conditional entropy of X given Z. Computing MI can be difficult without knowing the marginal and joint probability distributions ($\mathbb{P}_{\mathbb{X}}$, $\mathbb{P}_{\mathbb{Z}}$, and $\mathbb{P}_{\mathbb{XZ}}$). For efficient computation, the mutual information neural estimator (MINE) with consistency guarantees is proposed in (Belghazi et al. 2018). Specifically, MINE aims to maximize the lower bound of the exact MI using a model parameterized by a neural network θ, defined as $I_\Theta(X,Z) \leq I(X,Z)$, where Θ is the space of feasible parameters of a neural network, and $I_\Theta(X,Z)$ is the neural information quantity defined as $I_\Theta(X,Z) = \sup_{\theta\in\Theta} \mathbb{E}_{\mathbb{P}_{XZ}}[T_\theta] - \log(\mathbb{E}_{\mathbb{P}_X \otimes \mathbb{P}_Z}[e^{T_\theta}])$. The function T_θ is parameterized by a neural network θ based on the Donsker-Varadhan representation theorem (Donsker and Varadhan 1983). MINE estimates the expectation of the quantities above by shuffling the samples from the joint distribution along the batch axis or using empirical samples $\{x_i, z_i\}_{i=1}^n$ from $\mathbb{P}_{\mathbb{XZ}}$ and $\mathbb{P}_{\mathbb{X}} \otimes \mathbb{P}_{\mathbb{Z}}$ (the product of marginals).

MINE has been successfully applied to improve representation learning (Hjelm et al. 2019; Zhu, Zhang, and Evans 2020) given a dataset. However, for the purpose of generating an adversarial example for a given data sample, the vanilla MINE is not applicable because it only applies to a batch of data samples (so that empirical data distributions can be used for computing MI estimates) but not to single data sample. To bridge this gap, we will propose two MINE-based sampling methods for single data sample in Section 3.1.

3 Methodology

3.1 MINE of Single Data Sample

Given a data sample x and its perturbed sample $x+\delta$, we construct an auxiliary distribution using their random samples or convolution outputs to compute MI via MINE as a similarity measure, which we denote as "per-sample MINE".

Random Sampling Using compressive sampling (Candès and Wakin 2008), we perform independent Gaussian sampling of a given sample x to obtain a batch of K compressed samples $\{x_k, (x+\delta)_k\}_{k=1}^K$ for computing $I_\Theta(x, x+\delta)$ via MINE. We refer the readers to the supplementary material (SuppMat 6.2, 6.3) for more details. We also note that random sampling is agnostic to the underlying machine learning model since it directly applies to the data sample.

Convolution Layer Output When the underlying neural network model uses a convolution layer to process the input

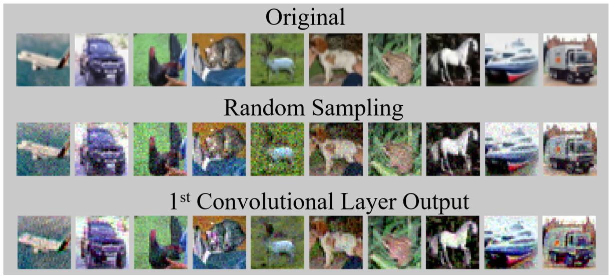

Figure 1: Visual comparison of MINE-based untargeted supervised adversarial examples (with $\epsilon = 1$) on CIFAR-10.

Per-sample MINE Method	FID	KID
Random Sampling (10 runs, $K = 96$)	339.47 ± 8.07	14.86 ± 1.45
1st Convolution Layer Output ($K = 96$)	344.231	10.78

Table 2: Frechet and kernel inception distances (FID/KID) between the untargeted adversarial examples of 1000 test samples and the training data in CIFAR-10.

data (which is an almost granted setting for image data), we propose to use the output of the first convolution layer of a data input, denoted by $conv(\cdot)$, to obtain K feature maps $\{conv(x)_k, conv(x+\delta)_k\}_{k=1}^K$ for computing $I_\Theta(x, x+\delta)$. We provide the detailed algorithm for convolution-based per-sample MINE in SuppMat 6.2.

Evaluation We use the CIFAR-10 dataset and the same neural network as in Section 4.2 to provide qualitative and quantitative evaluations on the two per-sample MINE methods for image classification. Figure 1 shows their visual comparisons, with the objective of finding the most similar perturbed sample (measured by MINE with the maximal scaled L_∞ perturbation bound $\epsilon = 1$) leading to misclassification. Both random sampling and convolution-based approaches can generate high-similarity prediction-evasive adversarial examples despite of large L_∞ perturbation.

Table 2 compares the Frechet inception distance (FID) (Heusel et al. 2017) and the kernel inception distance (KID) (Bińkowski et al. 2018) between the generated adversarial examples versus the training data (lower value is better). Both per-sample MINE methods have comparable scores. The convolution-based approach attains lower KID score and is observed to have better visual quality as shown in Figure 1. We also tested the performance using the second convolution layer output but found degraded performance. In this paper we use convolution-based approach whenever applicable and otherwise use random sampling.

3.2 MINE-based Attack Formulation

We formalize the objectives for supervised/unsupervised adversarial examples using per-sample MINE. As summarized in Table 1, the supervised setting aims to find *most similar* examples causing prediction evasion, leading to an MINE *maximization* problem. The unsupervised setting aims to find *least similar* examples but having smaller training loss, leading to an MINE *minimization* problem. Both problems can be solved efficiently using our unified MinMax algorithm.

Let (x, y) denote a pair of a data sample x and its ground-truth label y. The objective of supervised adversarial example is to find a perturbation δ to x such that the MI estimate $I_\Theta(x, x+\delta)$ is maximized while the prediction of $x+\delta$ is different from y (or being a targeted class $y' \neq y$), which is formulated as

$$\underset{\delta}{\text{Maximize}} \quad I_\Theta(x, x+\delta)$$

such that $x + \delta \in [0,1]^d$, $\delta \in [-\epsilon, \epsilon]^d$ and $f_x(x+\delta) \leq 0$.

The constraint $x+\delta \in [0,1]^d$ ensures $x+\delta$ lies in the (normalized) data space of dimension d, and the constraint $\delta \in [-\epsilon, \epsilon]^d$ corresponds to the typical bounded L_∞ perturbation norm. We include this bounded-norm constraint to make direct comparisons to other norm-bounded attacks. One can ignore this constraint by setting $\epsilon = 1$. Finally, the function $f_x^{\text{sup}}(x+\delta)$ is an attack success evaluation function, where $f_x^{\text{sup}}(x+\delta) \leq 0$ means $x+\delta$ is a prediction-evasive adversarial example. For untargeted attack one can use the attack function f_x^{sup} designed in (Carlini and Wagner 2017b), which is $f_x^{\text{sup}}(x') = \text{logit}(x')_y - \max_{j:j\neq y} \text{logit}(x')_j + \kappa$, where $\text{logit}(x')_j$ is the j-th class output of the logit (pre-softmax) layer of a neural network, and $\kappa \geq 0$ is a tunable gap between the original prediction $\text{logit}(x')_y$ and the top prediction $\max_{j:j\neq y} \text{logit}(x')_j$ of all classes other than y. Similarly, the attack function for targeted attack with a class label $y' \neq y$ is $f_x^{\text{sup}}(x') = \max_{j:j\neq y'} \text{logit}(x')_j - \text{logit}(x')_{y'} + \kappa$.

Unsupervised Adversarial Example Many machine learning tasks such as data reconstruction and unsupervised representation learning do not use data labels, which prevents the use of aforementioned supervised attack functions. Here we use an autoencoder $\Phi(\cdot)$ for data reconstruction to illustrate the unsupervised attack formulation. The design principle can naturally extend to other unsupervised tasks. The autoencoder Φ takes a data sample x as an input and outputs a reconstructed data sample $\Phi(x)$. Different from the rationale of supervised attack, for unsupervised attack we propose to use MINE to find the *least similar* perturbed data sample $x+\delta$ with respect to x while ensuring the reconstruction loss of $\Phi(x+\delta)$ is no greater than $\Phi(x)$ (i.e., the criterion of successful attack for data reconstruction). The unsupervised attack formulation is as follows:

$$\underset{\delta}{\text{Minimize}} \quad I_\Theta(x, x+\delta)$$

such that $x + \delta \in [0,1]^d$, $\delta \in [-\epsilon, \epsilon]^d$ and $f_x(x+\delta) \leq 0$

The first two constraints regulate the feasible data space and the perturbation range. For the L_2-norm reconstruction loss, the unsupervised attack function is

$$f_x^{\text{unsup}}(x+\delta) = \|x - \Phi(x+\delta)\|_2 - \|x - \Phi(x)\|_2 + \kappa$$

which means the attack is successful (i.e., $f_x^{\text{unsup}}(x+\delta) \leq 0$) if the reconstruction loss of $x+\delta$ relative to the original sample x is smaller than the native reconstruction loss minus a nonnegative margin κ. That is, $\|x - \Phi(x+\delta)\|_2 \leq$

$\|x - \Phi(x)\|_2 - \kappa$. In other words, our unsupervised attack formulation aims to find that most dissimilar perturbed sample $x + \delta$ to x measured by MINE while having smaller reconstruction loss (in reference to x) than x. Such UAEs thus relates to generalization errors on low-loss samples because the model is biased toward these unseen samples.

3.3 MINE-based Attack Algorithm

Here we propose a unified MinMax algorithm for solving the aforementioned supervised and unsupervised attack formulations, and provide its convergence proof in Section 3.4. For simplicity, we will use f_x to denote the attack criterion for f_x^{sup} or f_x^{unsup}. Without loss of generality, we will analyze the supervised attack objective of maximizing I_Θ with constraints. The analysis also holds for the unsupervised case since minimizing I_Θ is equivalent to maximizing I'_Θ, where $I'_\Theta = -I_\Theta$. We will also discuss a penalty-based algorithm as a comparative method to our proposed approach.

MinMax Algorithm (proposed) We reformulate the attack generation via MINE as the following MinMax optimization problem with simple convex set constraints:

$$\underset{\delta: x+\delta \in [0,1]^d,\ \delta \in [-\epsilon,\epsilon]^d}{\text{Min}} \ \underset{c \geq 0}{\text{Max}} \quad F(\delta, c) \triangleq c \cdot f_x^+(x+\delta) - I_\Theta(x, x+\delta)$$

The outer minimization problem finds the best perturbation δ with data and perturbation feasibility constraints $x + \delta \in [0,1]^d$ and $\delta \in [-\epsilon, \epsilon]^d$, which are both convex sets with known analytical projection functions. The inner maximization associates a variable $c \geq 0$ with the original attack criterion $f_x(x + \delta) \leq 0$, where c is multiplied to the ReLU activation function of f_x, denoted as $f_x^+(x + \delta) = \text{ReLU}(f_x(x + \delta)) = \max\{f_x(x + \delta), 0\}$. The use of f_x^+ means when the attack criterion is not met (i.e., $f_x(x + \delta) > 0$), the loss term $c \cdot f_x(x + \delta)$ will appear in the objective function F. On the other hand, if the attack criterion is met (i.e., $f_x(x + \delta) \leq 0$), then $c \cdot f_x^+(x + \delta) = 0$ and the objective function F only contains the similarity loss term $-I_\Theta(x, x + \delta)$. Therefore, the design of f_x^+ balances the tradeoff between the two loss terms associated with attack success and MINE-based similarity. We propose to use alternative projected gradient descent between the inner and outer steps to solve the MinMax attack problem, which is summarized in Algorithm 1. The parameters α and β denote the step sizes of the minimization and maximization steps, respectively. The gradient $\nabla f_x^+(x + \delta)$ with respect to δ is set to be 0 when $f_x(x + \delta) \leq 0$. Our MinMax algorithm returns the successful adversarial example $x + \delta^*$ with the best MINE value $I_\Theta^*(x, x + \delta^*)$ over T iterations.

Penalty-based Algorithm (baseline) An alternative approach to solving the MINE-based attack formulation is the penalty-based method with the objective:

$$\underset{\delta: x+\delta \in [0,1]^d,\ \delta \in [-\epsilon,\epsilon]^d}{\text{Minimize}} \quad c \cdot f_x^+(x+\delta) - I_\Theta(x, x+\delta)$$

where c is a fixed regularization coefficient instead of an optimization variable. Prior arts such as (Carlini and Wagner 2017b) use a binary search strategy for tuning c and report the best attack results among a set of c values. In contrast, our MinMax attack algorithm dynamically adjusts the c value in the inner maximization stage (step 8 in Algorithm 1). In

Algorithm 1: MinMax Attack Algorithm

1: **Require:** data sample x, attack criterion $f_x(\cdot)$, step sizes α and β, perturbation bound ϵ, # of iterations T
2: Initialize $\delta_0 = 0$, $c_0 = 0$, $\delta^* =$ null, $I_\Theta^* = -\infty$, $t = 1$
3: **for** t in T iterations **do**
4: $\quad \delta_{t+1} = \delta_t - \alpha \cdot (c \cdot \nabla f_x^+(x + \delta_t) - \nabla I_\Theta(x, x + \delta_t))$
5: $\quad$ Project δ_{t+1} to $[-\epsilon, \epsilon]$ via clipping
6: $\quad$ Project $x + \delta_{t+1}$ to $[0, 1]$ via clipping
7: $\quad$ Compute $I_\Theta(x, x + \delta_{t+1})$
8: $\quad$ Perform $c_{t+1} = (1 - \frac{\beta}{t^{1/4}}) \cdot c_t + \beta \cdot f_x^+(x + \delta_{t+1})$
9: $\quad$ Project c_{t+1} to $[0, \infty]$
10: $\quad$ **if** $f_x(x+\delta_{t+1}) \leq 0$ and $I_\Theta(x, x+\delta_{t+1}) > I_\Theta^*$ **then**
11: $\quad\quad$ update $\delta^* = \delta_{t+1}$ and $I_\Theta^* = I_\Theta(x, x + \delta_{t+1})$
12: **Return** δ^*, I_Θ^*

Section 4.2, we will show that our MinMax algorithm is more efficient in finding MINE-based adversarial examples than the penalty-based algorithm. The details of the binary search process are given in SuppMat 6.5. Both methods have similar computation complexity involving T iterations of gradient and MINE computations.

3.4 Convergence Proof of MinMax Attack

As a theoretical justification of our proposed MinMax attack algorithm (Algorithm 1), we provide a convergence proof with the following assumptions on the considered problem:

• **A.1:** The feasible set Δ for δ is compact, and $f_x^+(x + \delta)$ has (well-defined) gradients and Lipschitz continuity (with respect to δ) with constants L_f and l_f. That is, $|f_x^+(x + \delta) - f_x^+(x + \delta')| \leq l_f \|\delta - \delta'\|$ and $\|\nabla f_x^+(x + \delta)) - \nabla f_x^+(x + \delta')\| \leq L_f \|\delta - \delta'\|,\ \forall\, \delta, \delta' \in \Delta$. Moreover, $I_\Theta(x, x + \delta)$ also has gradient Lipschitz continuity with constant L_I.

• **A.2:** The per-sample MINE is η-stable over iterations for the same input, $|I_{\Theta_{t+1}}(x, x + \delta_{t+1}) - I_{\Theta_t}(x, x + \delta_{t+1})| \leq \eta$.

A.1 holds in general for neural networks since the numerical gradient of ReLU activation can be efficiently computed and the sensitivity (Lipschitz constant) against the input perturbation can be bounded (Weng et al. 2018). The feasible perturbation set Δ is compact when the data space is bounded. A.2 holds by following the consistent estimation proof of the native MINE in (Belghazi et al. 2018).

To state our main theoretical result, we first define the proximal gradient of the objective function as $\mathcal{L}(\delta, c) := [\delta - P_\Delta[\delta - \nabla_\delta F(\delta, c)], c - P_\mathcal{C}[c + \nabla_c F(\delta, c)]]$, where $P_\mathcal{X}$ denotes the projection operator on convex set $\mathcal{X}$, and $\|\mathcal{L}(\delta, c)\|$ is a commonly used measure for stationarity of the obtained solution. In our case, $\Delta = \{\delta : x + \delta \in [0,1]^d \cap \delta \in [-\epsilon, \epsilon]^d\}$ and $\mathcal{C} = \{c : 0 \leq c \leq \bar{c}\}$, where $\bar{c}$ can be an arbitrary large value. When $\|\mathcal{L}(\delta^*, c^*)\| = 0$, then the point (δ^*, c^*) is refereed as a game stationary point of the min-max problem (Razaviyayn et al. 2020). Next, we now present our main theoretical result.

Theorem 1. *Suppose Assumptions A.1 and A.2 hold and the sequence $\{\delta_t, c_t, \forall t \geq 1\}$ is generated by the MinMax attack algorithm. For a given small constant*

ε' and positive constant β, let $T(\varepsilon')$ denote the first iteration index such that the following inequality is satisfied: $T(\varepsilon') := \min\{t | \|\mathcal{L}(\delta_t, c_t)\|^2 \leq \varepsilon', t \geq 1\}$. Then, when the step-size and approximation error achieved by Algorithm 1 satisfy $\alpha \sim \eta \sim \sqrt{1/T(\varepsilon')}$, there exists some constant C such that $\|\mathcal{L}(\delta_{T(\varepsilon')}, c_{T(\varepsilon')})\|^2 \leq C/\sqrt{T(\varepsilon')}$.

Proof. Please see the supplemental material (SuppMat 6.8).

Theorem 1 states the rate of convergence of our proposed MinMax attack algorithm when provided with sufficient stability of MINE and proper selection of the step sizes. We also remark that under the assumptions and conditions of step-sizes, this convergence rate is standard in non-convex min-max saddle point problems (Lu et al. 2020).

3.5 Data Augmentation Using UAE

With the proposed MinMax attack algorithm and per-sample MINE for similarity evaluation, we can generate MINE-based supervised and unsupervised adversarial examples (UAEs). Section 4 will show novel applications of MINE-based UAEs as a simple plug-in data augmentation tool to boost the model performance of several unsupervised machine learning tasks. We observe significant and consistent performance improvement in data reconstruction (up to 73.5% improvement), representation learning (up to 1.39% increase in accuracy), and contrastive learning (1.58% increase in accuracy). The observed performance gain can be attributed to the fact that our UAEs correspond to "on-manifold" data samples having low training loss but are dissimilar to the training data, causing generalization errors. Therefore, data augmentation and retraining with UAEs can improve generalization (Stutz, Hein, and Schiele 2019).

4 Performance Evaluation

In this section, we conduct extensive experiments on a variety of datasets and neural network models to demonstrate the performance of our proposed MINE-based MinMax adversarial attack algorithm and the utility of its generated UAEs for data augmentation, where a high attack success rate using UAEs suggests rich space for data augmentation to improve model performance. Codes are available at https://github.com/IBM/UAE.

4.1 Experiment Setup and Datasets

Datasets and Computing Resource We provide a brief summary of the datasets and computing resource in SuppMat 6.18.

Supervised Adversarial Example Setting Both data samples and their labels are used in the supervised setting. We select 1000 test images classified correctly by the pretrained MNIST and CIFAR-10 deep neural network classifiers used in (Carlini and Wagner 2017b) and set the confidence gap parameter $\kappa = 0$ for the designed attack function f_x^{sup} defined in Section 3.2. The attack success rate (ASR) is the fraction of the final perturbed samples leading to misclassification.

Unsupervised Adversarial Example Setting Only the training data samples are used in the unsupervised setting. Their true labels are used in the post-hoc analysis for evaluating the quality of the associated unsupervised learning tasks. All training data are used for generating UAEs individually by setting $\kappa = 0$. A perturbed data sample is considered as a successful attack if its loss (relative to the original sample) is no greater than the original training loss (see Table 1). For data augmentation, if a training sample fails to find a successful attack, we will replicate itself to maintain data balance. The ASR is measured on the training data, whereas the reported model performance is evaluated on the test data. The training performance is provided in SuppMat 6.10.

MinMax Algorithm Parameters We use consistent parameters by setting $\alpha = 0.01$, $\beta = 0.1$, and $T = 40$ as the default values. The vanilla MINE model (Belghazi et al. 2018) is used in our per-sample MINE implementation.

Models and Codes We defer the summary of the considered machine learning models to the corresponding sections.

	MNIST		CIFAR-10	
	ASR	MI	ASR	MI
Penalty-based	100%	28.28	100%	13.69
MinMax	100%	**51.29**	100%	**17.14**

Table 3: Comparison between MinMax and penality-based algorithms on MNIST and CIFAR-10 datasets in terms of attack success rate (ASR) and mutual information (MI) value averaged over 1000 adversarial examples.

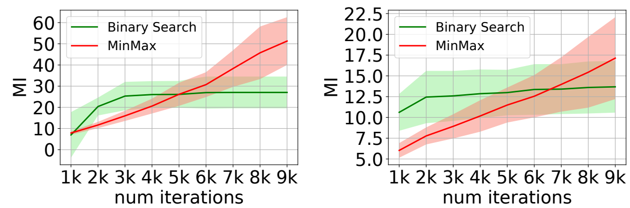

(a) MNIST (b) CIFAR-10

Figure 2: Mean and standard deviation of mutual information (MI) value versus attack iteration over 1000 samples.

4.2 MinMax v.s. Penalty-based Algorithms

We use the same untargeted supervised attack formulation and a total of $T = 9000$ iterations to compare our proposed MinMax algorithm with the penalty-based algorithm using 9 binary search steps on MNIST and CIFAR-10. Table 3 shows that while both methods can achieve 100% ASR, MinMax algorithm attains much higher MI values than penalty-based algorithm. The results show that the MinMax approach is more efficient in finding MINE-based adversarial examples, which can be explained by the dynamic update of the coefficient c in Algorithm 1.

Figure 2 compares the statistics of MI values over attack iterations. One can find that as iteration count increases, MinMax algorithm can continue improving the MI value, whereas penalty-based algorithm saturates at a lower MI value due to the use of fixed coefficient c in the attack process. In the remaining experiments, we will report the results using MinMax algorithm due to its efficiency.

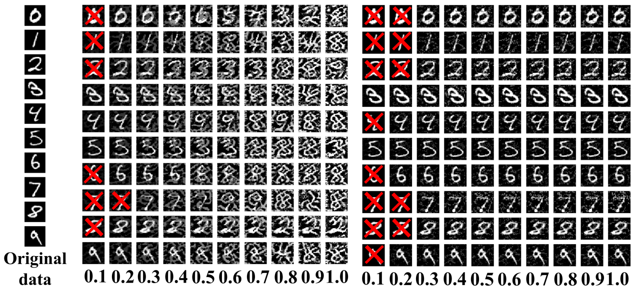

(a) (b) PGD attack (c) MinMax attack

Figure 3: Comparison of untargeted supervised adversarial examples on MNIST. The unsuccessful adversarial examples are marked with red crosses. Each column corresponds to different ϵ values (L_∞-norm perturbation bound) ranging from 0.1 to 1.0. Each row shows the adversarial examples of an original sample. MinMax attack using MINE yields adversarial examples with better visual quality than PGD attack, especially for large ϵ values.

4.3 Qualitative Visual Comparison

Figure 3 presents a visual comparison of MNIST supervised adversarial examples crafted by MinMax attack and the PGD attack with 100 iterations (Madry et al. 2018) given different ϵ values governing the L_∞ perturbation bound. The main difference is that MinMax attack uses MINE as an additional similarity regulation while PGD attack only uses L_∞ norm. Given the same ϵ value, MinMax attack yields adversarial examples with better visual quality. The results validate the importance of MINE as an effective similarity metric. In contrast, PGD attack aims to make full use of the L_∞ perturbation bound and attempts to modify every data dimension, giving rise to lower-quality adversarial examples. Similar results are observed for adversarially robust models (Madry et al. 2018; Zhang et al. 2019), as shown in SuppMat 6.16.

Moreover, the results also suggest that for MINE-based attacks, the L_∞ norm constraint on the perturbation is not critical for the resulting visual quality, which can be explained by the fact that MI is a fundamental information-theoretic similarity measure. When performing MINE-based attacks, we suggest not using the L_∞ norm constraint (by setting $\epsilon = 1$) so that the algorithm can fully leverage the power of MI to find a more diverse set of adversarial examples.

Next, we study three different unsupervised learning tasks. We only use the training samples and the associated training loss to generate UAEs. The post-hoc analysis reports the performance on the test data and the downstream classification accuracy. We report their improved adversarial robustness after data augmentation with MINE-UAEs in SuppMat 6.17.

4.4 UAE Improves Data Reconstruction

Data reconstruction using an autoencoder $\Phi(\cdot)$ that learns to encode and decode the raw data through latent representations is a standard unsupervised learning task. Here we use the default implementation of the following four autoencoders to generate UAEs based on the training data samples of MNIST and SVHN for data augmentation, retrain the model from scratch on the augmented dataset, and report the resulting reconstruction error on the original test set.

We also compare the performance of our proposed MINE-based UAE (MINE-UAE) with two baselines: (i) L_2-*UAE* that replaces the objective of minimizing $I_\Theta(x, x+\delta)$ with maximizing the L_2 reconstruction loss $\|x - \Phi(x+\delta)\|_2$ in the MinMax attack algorithm while keeping the same attack success criterion; (ii) *Gaussian augmentation* (GA) that adds zero-mean Gaussian noise with a diagonal covariance matrix of the same constant σ^2 to the training data.

Table 4 shows the reconstruction loss and the ASR. The improvement of reconstruction error is measured with respect to the reconstruction loss of the original model (i.e., without data augmentation). We find that MINE-UAE can attain much higher ASR than L_2-UAE and GA in most cases. More importantly, data augmentation using MINE-UAE achieves consistent and significant reconstruction performance improvement across all models and datasets (up to 56.7% on MNIST and up to 73.5% on SVHN), validating the effectiveness of MINE-UAE for data augmentation. On the other hand, in several cases L_2-UAE and GA lead to notable performance degradation. The results suggest that MINE-UAE can be an effective plug-in data augmentation tool for boosting the performance of unsupervised machine learning models.

4.5 UAE Improves Representation Learning

The concrete autoencoder (Balın, Abid, and Zou 2019) is an unsupervised feature selection method which recognizes a subset of the most informative features through an additional *concrete select layer* with M nodes in the encoder for data reconstruction. We apply MINE-UAE for data augmentation and use the same post-hoc classification evaluation procedure as in (Balın, Abid, and Zou 2019).

The six datasets and the resulting classification accuracy are reported in Table 6. We select $M = 50$ features for every dataset except for Mice Protein (we set $M = 10$) owing to its small data dimension. MINE-UAE can attain up to 11% improvement for data reconstruction and up to 1.39% increase in accuracy among 5 out of 6 datasets, corroborating the utility of MINE-UAE in representation learning and feature selection. The exception is Coil-20. A closer inspection shows that MINE-UAE has low ASR ($<10\%$) for Coil-20 and the training loss after data augmentation is significantly higher than the original training loss (see SuppMat 6.10). Therefore, we conclude that the degraded performance in Coil-20 after data augmentation is likely due to the limitation of feature selection protocol and the model learning capacity.

4.6 UAE Improves Contrastive Learning

The SimCLR algorithm (Chen et al. 2018) is a popular contrastive learning framework for visual representations. It uses self-supervised data modifications to efficiently improve several downstream image classification tasks. We use the default implementation of SimCLR on CIFAR-10 and generate MINE-UAEs using the training data and the defined training loss for SimCLR. Table 5 shows the loss, ASR and the resulting classification accuracy by taining a linear head on the learned representations. We find that using MINE-UAE for

MNIST									
	Reconstruction Error (test set)					ASR (training set)			
Autoencoder	Original	MINE-UAE	L_2-UAE	GA ($\sigma = 0.01$)	GA ($\sigma = 10^{-3}$)	MINE-UAE	L_2-UAE	GA ($\sigma = 0.01$)	GA ($\sigma = 10^{-3}$)
Sparse	0.00561	**0.00243** ($\uparrow$ 56.7%)	0.00348 ($\uparrow$ 38.0%)	0.00280±2.60e-05 ($\uparrow$ 50.1%)	0.00280±3.71e-05 ($\uparrow$ 50.1%)	100%	99.18%	54.10%	63.95%
Dense	0.00258	**0.00228** ($\uparrow$ 11.6%)	0.00286 ($\downarrow$ 6.0%)	0.00244±0.00014 ($\uparrow$ 5.4%)	0.00238±0.00012 ($\uparrow$ 7.8%)	92.99%	99.94%	48.53%	58.47%
Convolutional	0.00294	**0.00256** ($\uparrow$ 12.9%)	0.00364 ($\downarrow$ 23.8%)	0.00301±0.00011 ($\downarrow$ 2.4%)	0.00304±0.00015 ($\downarrow$ 3.4%)	99.86%	99.61%	68.71%	99.61%
Adversarial	0.04785	**0.04581** ($\uparrow$ 4.3%)	0.06098 ($\downarrow$ 27.4%)	0.05793±0.00501 ($\downarrow$ 21%)	0.05544±0.00567 ($\downarrow$ 15.86%)	98.46%	43.54%	99.79%	99.83%
SVHN									
Sparse	0.00887	**0.00235** ($\uparrow$ 73.5%)	0.00315 ($\uparrow$ 64.5%)	0.00301±0.00137 ($\uparrow$ 66.1%)	0.00293±0.00078 ($\uparrow$ 67.4%)	100%	72.16%	72.42%	79.92%
Dense	0.00659	**0.00421** ($\uparrow$ 36.1%)	0.00550 ($\uparrow$ 16.5%)	0.00858±0.00232 ($\downarrow$ 30.2%)	0.00860±0.00190 ($\downarrow$ 30.5%)	99.99%	82.65%	92.3%	93.92%
Convolutional	0.00128	**0.00095** ($\uparrow$ 25.8%)	0.00121 ($\uparrow$ 5.5%)	0.00098 ± 3.77e-05 ($\uparrow$ 25.4%)	0.00104±7.41e-05 ($\uparrow$ 18.8%)	100%	56%	96.40%	99.24%
Adversarial	0.00173	**0.00129** ($\uparrow$ 25.4%)	0.00181 ($\downarrow$ 27.4%)	0.00161±0.00061 ($\uparrow$ 6.9%)	0.00130±0.00037 ($\uparrow$ 24.9%)	94.82%	58.98%	97.31%	99.85%

Table 4: Comparison of data reconstruction by retraining the autoencoder on UAE-augmented data. The error is the average L_2 reconstruction loss of the test set. The improvement is relative to the original model. The attack success rate (ASR) is the fraction of augmented training data having smaller reconstruction loss than the original loss (see Table 1 for definition).

CIFAR-10			
Model	Loss (test set)	Accuracy (test set)	ASR
Original	0.29010	91.30%	-
MINE-UAE	**0.26755** ($\uparrow$ 7.8%)	**+1.58%**	100%
CLAE	-	+0.05%	-

Table 5: Comparison of contrastive loss and the resulting accuracy on CIFAR-10 using SimCLR (Chen et al. 2018) (ResNet-18 with batch size = 512). The attack success rate (ASR) is the fraction of augmented training data having smaller contrastive loss than original loss. For CLAE (Ho and Vasconcelos 2020), we use the reported accuracy improvement (it shows negative gain in our implementation), though its base SimCLR model only has 83.27% test accuracy.

additional data augmentation and model retraining can yield 7.8% improvement in contrastive loss and 1.58% increase in classification accuracy. Comparing to (Ho and Vasconcelos 2020) using adversarial examples to improve SimCLR (named CLAE), the accuracy increase of MINE-UAE is 30x higher. Moreover, MINE-UAE data augmentation also significantly improves adversarial robustness (see SuppMat 6.17).

5 Conclusion

In this paper, we propose a novel framework for studying adversarial examples in unsupervised learning tasks, based on our developed per-sample mutual information neural estimator as an information-theoretic similarity measure. We also

	Recons. Error (test set)		Accuracy (test set)	
Dataset	Original	MINE-UAE	Original	MINE-UAE
MNIST	0.01170	**0.01142** ($\uparrow$ 2.4%)	94.97%	95.41%
Fashion MMIST	0.01307	**0.01254** ($\uparrow$ 4.1%)	84.92%	85.24%
Isolet	0.01200	**0.01159** ($\uparrow$ 3.4%)	81.98%	82.93%
Coil-20	**0.00693**	0.01374 ($\downarrow$ 98.3%)	98.96%	96.88%
Mice Protein	0.00651	**0.00611** ($\uparrow$ 6.1%)	89.81%	91.2%
Activity	0.00337	**0.00300** ($\uparrow$ 11.0%)	83.38%	84.45%

Table 6: Performance of representation learning by the concrete autoencoder and the resulting classification accuracy. The degradation on Coil-20 is explained in Section 4.5.

propose a new MinMax algorithm for efficient generation of MINE-based supervised and unsupervised adversarial examples and establish its convergence guarantees. As a novel application, we show that MINE-based UAEs can be used as a simple yet effective plug-in data augmentation tool and achieve significant performance gains in data reconstruction, representation learning, and contrastive learning.

Acknowledgments

This work was primarily done during Chia-Yi's visit at IBM Research. Chia-Yi Hsu and Chia-Mu Yu were supported by

MOST 110-2636-E-009-018, and we also thank National Center for High-performance Computing (NCHC) of National Applied Research Laboratories (NARLabs) in Taiwan for providing computational and storage resources.

References

Athalye, A.; Carlini, N.; and Wagner, D. 2018. Obfuscated gradients give a false sense of security: Circumventing defenses to adversarial examples. *International Coference on International Conference on Machine Learning*.

Balın, M. F.; Abid, A.; and Zou, J. 2019. Concrete autoencoders: Differentiable feature selection and reconstruction. In *International Conference on Machine Learning*, 444–453.

Belghazi, M. I.; Baratin, A.; Rajeshwar, S.; Ozair, S.; Bengio, Y.; Courville, A.; and Hjelm, D. 2018. Mutual information neural estimation. In *International Conference on Machine Learning*, 531–540.

Biggio, B.; and Roli, F. 2018. Wild patterns: Ten years after the rise of adversarial machine learning. *Pattern Recognition*, 84: 317–331.

Bińkowski, M.; Sutherland, D. J.; Arbel, M.; and Gretton, A. 2018. Demystifying MMD GANs. In *International Conference on Learning Representations*.

Brendel, W.; Rauber, J.; and Bethge, M. 2018. Decision-Based Adversarial Attacks: Reliable Attacks Against Black-Box Machine Learning Models. *International Conference on Learning Representations*.

Candès, E. J.; and Wakin, M. B. 2008. An introduction to compressive sampling. *IEEE Signal Processing Magazine*, 25(2): 21–30.

Carlini, N.; and Wagner, D. 2017a. Adversarial examples are not easily detected: Bypassing ten detection methods. In *ACM Workshop on Artificial Intelligence and Security*, 3–14.

Carlini, N.; and Wagner, D. 2017b. Towards evaluating the robustness of neural networks. In *IEEE Symposium on Security and Privacy*, 39–57.

Carmon, Y.; Raghunathan, A.; Schmidt, L.; Liang, P.; and Duchi, J. C. 2019. Unlabeled data improves adversarial robustness. *Neural Information Processing Systems*.

Cemgil, T.; Ghaisas, S.; Dvijotham, K. D.; and Kohli, P. 2020. Adversarially Robust Representations with Smooth Encoders. In *International Conference on Learning Representations*.

Chen, P.-Y.; Zhang, H.; Sharma, Y.; Yi, J.; and Hsieh, C.-J. 2017. ZOO: Zeroth Order Optimization Based Black-box Attacks to Deep Neural Networks Without Training Substitute Models. In *ACM Workshop on Artificial Intelligence and Security*, 15–26.

Chen, T.; Kornblith, S.; Norouzi, M.; and Hinton, G. 2018. A simple framework for contrastive learning of visual representations. In *International Conference on Machine Learning*.

Donsker, M. D.; and Varadhan, S. S. 1983. Asymptotic evaluation of certain Markov process expectations for large time. IV. *Communications on Pure and Applied Mathematics*, 36(2): 183–212.

Goodfellow, I. J.; Shlens, J.; and Szegedy, C. 2015. Explaining and harnessing adversarial examples. *International Conference on Learning Representations*.

Heusel, M.; Ramsauer, H.; Unterthiner, T.; Nessler, B.; and Hochreiter, S. 2017. Gans trained by a two time-scale update rule converge to a local nash equilibrium. In *Advances in Neural Information Processing Systems*, 6626–6637.

Hjelm, R. D.; Fedorov, A.; Lavoie-Marchildon, S.; Grewal, K.; Bachman, P.; Trischler, A.; and Bengio, Y. 2019. Learning deep representations by mutual information estimation and maximization. In *International Conference on Learning Representations*.

Ho, C.-H.; and Vasconcelos, N. 2020. Contrastive learning with adversarial examples. In *Advances in Neural Information Processing Systems*.

Liu, S.; Lu, S.; Chen, X.; Feng, Y.; Xu, K.; Al-Dujaili, A.; Hong, M.; and O'Reilly, U.-M. 2020. Min-max optimization without gradients: Convergence and applications to black-box evasion and poisoning attacks. In *International Conference on Machine Learning*.

Lu, S.; Tsaknakis, I.; Hong, M.; and Chen, Y. 2020. Hybrid Block Successive Approximation for One-Sided Non-Convex Min-Max Problems: Algorithms and Applications. *IEEE Transactions on Signal Processing*, 68: 3676–3691.

Madry, A.; Makelov, A.; Schmidt, L.; Tsipras, D.; and Vladu, A. 2018. Towards Deep Learning Models Resistant to Adversarial Attacks. *International Conference on Learning Representations*.

Miyato, T.; Maeda, S.-i.; Koyama, M.; and Ishii, S. 2018. Virtual adversarial training: a regularization method for supervised and semi-supervised learning. *IEEE transactions on pattern analysis and machine intelligence*, 41(8): 1979–1993.

Nitin Bhagoji, A.; He, W.; Li, B.; and Song, D. 2018. Practical Black-box Attacks on Deep Neural Networks using Efficient Query Mechanisms. In *Proceedings of the European Conference on Computer Vision (ECCV)*, 154–169.

Papernot, N.; McDaniel, P.; Goodfellow, I.; Jha, S.; Celik, Z. B.; and Swami, A. 2017. Practical black-box attacks against machine learning. In *ACM Asia Conference on Computer and Communications Security*, 506–519.

Ranzato, M.; Huang, F. J.; Boureau, Y.-L.; and LeCun, Y. 2007. Unsupervised learning of invariant feature hierarchies with applications to object recognition. In *IEEE Conference on Computer Vision and Pattern Recognition*, 1–8.

Razaviyayn, M.; Huang, T.; Lu, S.; Nouiehed, M.; Sanjabi, M.; and Hong, M. 2020. Nonconvex Min-Max Optimization: Applications, Challenges, and Recent Theoretical Advances. *IEEE Signal Processing Magazine*, 37(5): 55–66.

Stanforth, R.; Fawzi, A.; Kohli, P.; et al. 2019. Are Labels Required for Improving Adversarial Robustness? *Neural Information Processing Systems*.

Stutz, D.; Hein, M.; and Schiele, B. 2019. Disentangling adversarial robustness and generalization. In *Proceedings of the IEEE Conference on Computer Vision and Pattern Recognition*, 6976–6987.

Su, D.; Zhang, H.; Chen, H.; Yi, J.; Chen, P.-Y.; and Gao, Y. 2018. Is robustness the cost of accuracy?–a comprehensive study on the robustness of 18 deep image classification models. In *Proceedings of the European Conference on Computer Vision (ECCV)*, 631–648.

Szegedy, C.; Zaremba, W.; Sutskever, I.; Bruna, J.; Erhan, D.; Goodfellow, I.; and Fergus, R. 2013. Intriguing properties of neural networks. *arXiv preprint arXiv:1312.6199*.

Tsipras, D.; Santurkar, S.; Engstrom, L.; Turner, A.; and Madry, A. 2019. Robustness may be at odds with accuracy. In *International Conference on Learning Representations*.

Weng, T.-W.; Zhang, H.; Chen, P.-Y.; Yi, J.; Su, D.; Gao, Y.; Hsieh, C.-J.; and Daniel, L. 2018. Evaluating the Robustness of Neural Networks: An Extreme Value Theory Approach. *International Conference on Learning Representations*.

Zhai, X.; Oliver, A.; Kolesnikov, A.; and Beyer, L. 2019. S4l: Self-supervised semi-supervised learning. In *Proceedings of the IEEE international Conference on Computer Vision*, 1476–1485.

Zhang, H.; Yu, Y.; Jiao, J.; Xing, E.; El Ghaoui, L.; and Jordan, M. 2019. Theoretically principled trade-off between robustness and accuracy. In *International Conference on Machine Learning*, 7472–7482.

Zhu, S.; Zhang, X.; and Evans, D. 2020. Learning Adversarially Robust Representations via Worst-Case Mutual Information Maximization. *International Coference on International Conference on Machine Learning*.

Zhu, X.; and Goldberg, A. B. 2009. Introduction to semi-supervised learning. *Synthesis Lectures on Artificial Intelligence and Machine Learning*, 3(1): 1–130.